Technical University of Denmark

Pulse-shaping mechanism in colliding-pulse mode-locked laser diodes

Bischoff, Svend; Sørensen, Mads Peter; Mørk, J.; Brorson, S. D.; Franck, T.; Nielsen, J. M.; Møller-Larsen, A.

DTU Library
Technical Information Center of Denmark

Pulse-shaping mechanism in colliding-pulse mode-locked laser diodes

S. Bischoff[a)] and M. P. Sørensen
Institute of Mathematical Modelling, The Technical University of Denmark, DK-2800 Lyngby, Denmark

J. Mørk, S. D. Brorson, T. Franck, J. M. Nielsen, and A. Møller-Larsen
Tele Danmark Research, Lyngsø Allé 2, DK-2970 Hørsholm, Denmark

The large signal dynamics of passively colliding pulse mode-locked laser diodes is studied. We derive a model which explains modelocking via the interplay of gain and loss dynamics; no bandwidth limiting element is necessary for pulse formation. It is found necessary to have both fast and slow absorber dynamics to achieve mode-locking. Significant chirp is predicted for pulses emitted from long lasers, in agreement with experiment. The pulse width shows a strong dependence on both cavity and saturable absorber length. © *1995 American Institute of Physics.*

Monolithic colliding-pulse mode-locked (CPM) quantum-well (QW) lasers have been shown to generate optical pulses in the pico- to sub-picosecond range with repetition frequencies from 16 to 350 GHz.[1,2] Several laboratories have demonstrated CPM laser operation[1–4] and system experiments[5] have shown the potential of the CPM laser as a pulse source for high-speed time-division multiplexed optical transmission systems. Despite this, the operation principles, in particular those determining the pulse width, have only received very modest attention.[6,7] In this letter we present numerical simulations of the CPM laser, including details of the carrier dynamics in the active regions. The results are in good agreement with experimental results. In contrast to conventional mode-locking theory[8] attributing the pulse width to an interplay between saturable absorption/gain (leading to pulse sharpening) and dispersion/bandwidth limiting (leading to broadening), we find that the pulse width is determined entirely by the interplay between the gain and absorber dynamics.

Our large signal model takes into account the spatial and temporal variations of the electrical field, material gain, and refractive index. The wave propagation equation for the right (A^+) and left (A^-) travelling electrical field envelope function is

$$\pm\frac{\partial A^\pm(z,t)}{\partial z} + \frac{1}{v_g}\frac{\partial A^\pm(z,t)}{\partial t} = \Gamma\left(\frac{g}{2} - i\Delta k\right)A^\pm(z,t)$$

$$-\frac{\alpha_{\text{int}}}{2}A^\pm(z,t) + \frac{\beta_{\text{sp}}BN_{\text{qw}}^2(z,t)}{2A^\pm(z,t)}, \tag{1}$$

where v_g is the group velocity, Γ is the confinement factor, α_{int} is the internal loss, and $\beta_{\text{sp}}BN_{\text{qw}}^2(z,t)$ accounts for spontaneous emission. The gain g and wave number change Δk depend on the carrier distribution,

$$g = a_N(n_c + \bar{n}_v - N_0) \tag{2a}$$

$$\Delta k = \frac{\omega_0}{c}\left(\frac{\partial n}{\partial N_{\text{qw}}}\Delta N_{\text{qw}} + \frac{\partial n}{\partial T_c}\Delta T_c\right) \tag{2b}$$

where n_c is the "local" (gain determining) carrier density in the conduction band at the optical transition energy,[9] N_{qw} is the density of carriers confined in the QW, and T_c is the carrier temperature. Group velocity dispersion has been neglected, since for pulses larger than a few hundred fs we estimate its contribution to be much smaller than the calculated broadening due to gain dynamics. ω_0 is the optical carrier frequency and c is the speed of light in vacuum. a_N is the maximum obtainable differential gain and N_0 is related to the density of states.[9] The derivatives of the refractive index n are related to the linewidth enhancement factors α_N and α_T. The rate equations for the material dynamics are

$$\frac{\partial N_D}{\partial t} = -\frac{N_D}{\tau_{\text{sweep}}} - \frac{M_{\text{qw}}L_{\text{qw}}}{L_D}\frac{\eta_C N_D - N_{\text{qw}}}{\tau_d} - \frac{N_D}{\tau_{s_D}}, \tag{3a}$$

$$\frac{\partial N_{\text{qw}}}{\partial t} = \frac{\eta_C N_D - N_{\text{qw}}}{\tau_d} - v_g g S - \frac{N_{\text{qw}}}{\tau_{s_{\text{qw}}}}, \tag{3b}$$

$$\frac{\partial T_c}{\partial t} = \left[\frac{\sigma_c}{k_B}\hbar\omega_0 + \left(T_c - \frac{E_{c,0}}{k_B}\right)\frac{g}{N_{\text{qw}}}\right]v_g g S - \frac{T_c - T_L}{\tau_{h,c}}, \tag{3c}$$

$$\frac{\partial n_c}{\partial t} = -\frac{n_c - \bar{n}_c}{\tau_{1c}} - v_g g S. \tag{3d}$$

Apart from the introduction of a carrier reservoir N_D in the barrier to account for the finite transport time τ_d across the separate confinement region,[10] these equations correspond to those given in Ref. 9 and were found to give a good explanation of ultrafast gain dynamics in laser amplifiers. Equation (3c) is written down for the case of the absorber, where the Fermi-Dirac distribution can be approximated by a Boltzmann distribution. Also, in the gain sections, the sweep out term $-N_D/\tau_{\text{sweep}}$ is replaced by $I/(eA_{\text{vol}}L_D)$, corresponding to injections of carriers into the carrier reservoir. Other parameters are M_{qw} the number of quantum wells, L_{qw} and L_D the width of the quantum wells and the carrier reservoir respectively. η_c is the ratio between the carrier density in the reservoir (N_D) and in the quantum wells (N_{qw}) at thermal equilibrium and T_L is the lattice temperature. τ_{s_D} and $\tau_{s_{\text{qw}}}$ are the carrier lifetimes for N_D and N_{qw} respectively. σ_c is the free carrier absorption cross section and S

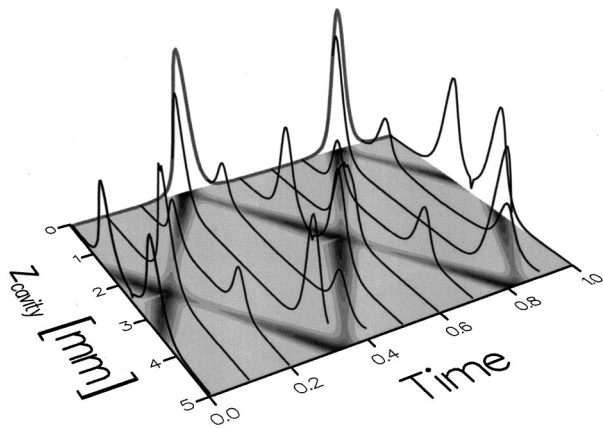
[a)]Electronic mail: sb@imm.dtu.dk

FIG. 1. Evolution of CPM pulses at steady state for a 5 mm long cavity with a 80 μm absorber. Snapshots of the intensity distribution along the cavity are shown during one roundtrip.

FIG. 3. Experimental and theoretical interferometric autocorrelation (a) and optical power spectrum (b) for a 5 mm laser diode (80 μm absorber).

($S=|A^+|^2+|A^-|^2$) is the photon density. k_B and $\hbar$ are the Boltzman and Planck constant. $E_{c,0}$ is the electron energy measured from the conduction band edge into the band. The local density n_c[11] approaches its quasiequilibrium value $\bar{n}_c=\bar{n}_c(N_{\mathrm{qw}},T_c)$ due to carrier-carrier scattering with a time constant $\tau_{1,c}$. The effect of carrier-carrier and carrier-phonon scattering has been neglected in the valence band [$\bar{n}_v=\bar{n}_v(N_{\mathrm{qw}},T_L)$].

Figure 1 shows an example of the computed steady-state CPM mode of operation for a 5 mm long laser diode with a 80 μm absorber. Important parameter values include $\alpha_N=3.0$, $\alpha_T=1.5$, $\tau_{1_{\mathrm{gain}}}=50$ fs, $\tau_{1_{\mathrm{abs}}}=100$ fs, $\tau_{d_{\mathrm{abs}}}=8$ ps and $\tau_{\mathrm{sweep}}=200$ fs. The output pulsewidth is 5.1 ps. As shown in the figure, the initial left-hand pulse travels toward the absorber, collides with the left propagating pulse in the absorber and continues toward the right-hand laser facet where it is reflected back into the laser. It is essential for mode-locking that the ratio between $\tau_{1_{\mathrm{abs}}}$ and $\tau_{1_{\mathrm{gain}}}$ is greater than one.

The changes in pulse width and amplitude during propagation inside the laser diode are displayed in Fig. 2. It is evident that the pulse broadens in the gain sections and is compressed in the absorber, and the steady-state pulses are
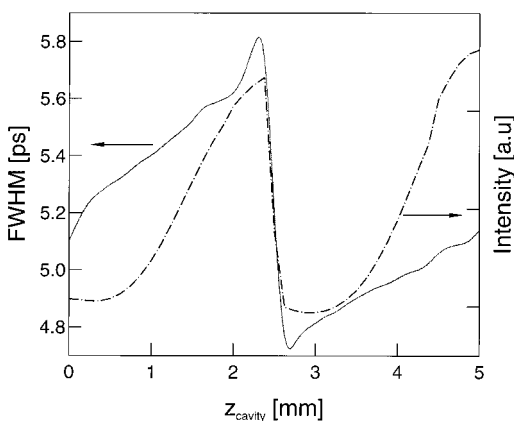

FIG. 2. Pulse width and amplitude displayed for the pulse traveling to the right for one pass through the laser diode.
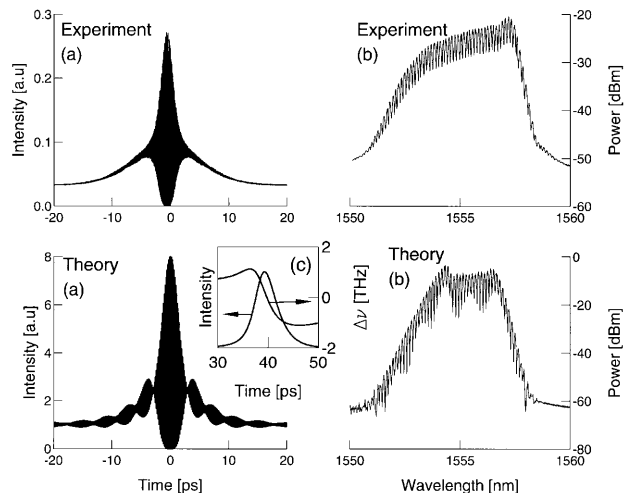
characterized by a balance between these opposite effects. This implies that the CPM is not an example of "pure slow saturable absorber" mode-locking,[8] since in that case, pulses are shortened by both gain and absorber sections. Rather, our model shows the necessity to have both slow and fast absorber recovery, where the slow absorber recovery is needed for self-starting. The fast absorber recovery is important for mode-locking. This is particularly true for short laser diodes (<3 mm), where the round trip time in the cavity can be shorter than the slow recovery time of semiconductor saturable absorbers (typically 4–16 ps depending on the applied reverse bias[12]). In these short structures, subpicosecond gain/absorption dynamics [spectral hole burning (SHB) and carrier heating/cooling] is instrumental for mode-locking. For longer cavities, where the pulse width is of the same magnitude as the recovery time of the saturable absorber, mode-locking can be achieved without including subpicosecond gain/absorption dynamics, but the effect of SHB in the gain/absorber has a big impact on the pulse width.[13]

The importance of carrier dynamics to mode-locking in our model differs significantly from that in Refs. 6 and 7. In their theory, mode-locking was related to the build up of a carrier density grating in the saturable absorber, and also relied on bandwidth limiting elements in the cavity, while these effects are not included in our model. Furthermore, they reported nearly transform limited pulses from long (2 mm) structures. Our model does not give transform limited pulses, but rather highly chirped pulses, which is in agreement with experimental measurements.[4] This is illustrated in Fig. 3, which shows calculated the interferometric autocorrelation and optical power spectrum as well as an example measurement of a hybrid mode-locked 5 mm long device.[4,5] The rising wings in the interferometric autocorrelation are a result of the strong downchirp of the pulse's instantaneous frequency, while the small oscillations in the wings of the theoretical interferometric autocorrelation is a result of the nonlinear chirp on the front edge and tail of the pulses. The inset in Fig. 3(c) shows the amplitude and frequency of the pulse. The almost linear downchirp on the pulse is mainly a
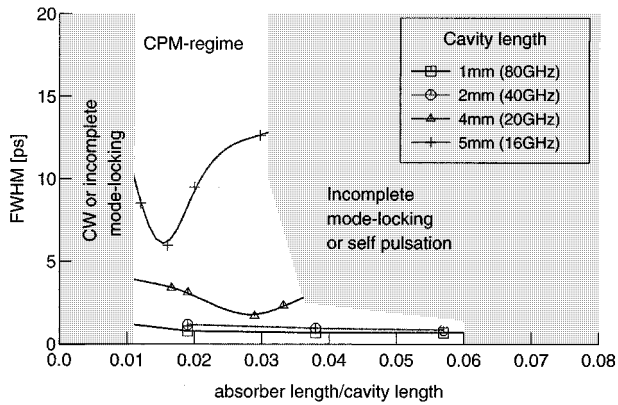
FIG. 4. Pulse width as function of absorber length for different cavity lengths. The thick lines represent approximate boundaries between the different operation regimes.

result of the carrier density induced index changes in the gain sections, but is somewhat reduced by carrier density changes in the saturable absorber. However, increasing the absorber length does not result in a reduction of the wavelength chirping, because the increased absorption must be compensated by an increase in amplification, which results in an overall increase in wavelength chirping. This is consistent with the general observation that pulses generated by long CPM laser diodes have a larger time-bandwidth product than pulses from short CPM laser diodes. Pulses, which are almost time-bandwidth limited, are found for small values of α_N. Thus, the chirp of the CPM pulses depends critically on the value of α_N as well as on a possible difference between α_N in the gain and the absorber section.

The model has been used to predict the behavior of the CPM laser for different cavity and absorber lengths. This is presented in Fig. 4, where the laser's operation state for four different cavity lengths (repetition frequencies) is shown as a function of the normalized absorber length. The injection current was adjusted between different cavity lengths in order to maintain an average output power on the order of 1 mW. The average output power decreases with increasing absorber length, which to some extent can be compensated

by increasing the injection current, resulting in pulse broadening.

Figure 4 shows that the absorber has to be below a certain length to prevent the laser from operating in the Q-switched/self-pulsing operation regime.[3,14] The repetition frequency in the Q-switched state for a 1 mm long laser diode is 10 GHz and decreases with increasing cavity length. The continuous wave (cw) solution is obtained when the saturable absorber becomes too short compared to the gain sections.

As depicted in Fig. 4, the region of good mode-locking is larger for short cavity structures, and becomes narrower for long laser diodes. We did not succeed in mode-locking a 10 GHz (very long cavity) CPM laser in our simulations. In agreement with experimental results,[1] the shortest CPM pulses are obtained for short cavities. Finally we find that the saturable absorber has an optimum length for a given current and absorber recovery time.

[1] Y. K. Chen and M. C. Wu, IEEE J. Quantum Electron. **28**, 2176 (1992).
[2] A. Møller-Larsen, Teleteknik **2**, 70 (1994).
[3] D. J. Derickson, R. J. Helkey, A. Mar, J. R. Karin, J. G. Wasserbauer, and J. E. Bowers, IEEE J. Quantum Electron **28**, 2186 (1992).
[4] S. D. Brorson, Z. Wang, T. Franck, S. Bischoff, A. Møller-Larsen, J. M. Nielsen, J. Mørk, and M. P. Sørensen, IEEE Photonics Technol. Lett. **7**, 1148 (1995).
[5] Z. Wang, J. M. Nielsen, S. D. Brorson, B. Christensen, T. Franck, A. Møller-Larsen, J. Nørregaard, and E. Bødtker, Electron. Lett. **31**, 272 (1995).
[6] L. M. Zhang and J. E. Carroll, IEEE J. Quantum Electron. **31**, 240 (1995).
[7] D. J. Jones, L. M. Zhang, J. E. Carroll, and D. D. Marcenac, IEEE J. Quantum Electron. **31**, 1051 (1995).
[8] H. A. Haus, IEEE J. Quantum Electron. **11**, 736 (1975).
[9] J. Mark and J. Mørk, Appl. Phys. Lett. **61**, 2281 (1992).
[10] N. Tessler and G. Eisenstein, IEEE J. Quantum Electron. **29**, 1586 (1993).
[11] M. Willatzen, J. Mark, J. Mørk, and C. P. Seltzer, Appl. Phys. Lett. **64**, 2206 (1994).
[12] J. R. Karin, R. J. Helkey, D. J. Derickson, R. Nagarajan, D. S. Allin, J. E. Bowers, and R. L. Thornton, Appl. Phys. Lett. **64**, 676 (1994).
[13] W. Yang and A. Gopinath, Appl. Phys. Lett. **63**, 2717 (1993).
[14] P. P. Vasil'ev, IEEE J. Quantum Electron. **29**, 1687 (1993).